Classical study of single-electron capture and ionization processes in $A^{q+}+(H,H_2)$ collisions

Clara Illescas and A. Riera
Departamento de Química, C-IX, Universidad Autónoma de Madrid, Cantoblanco, E-28049 Madrid, Spain
(Received 17 May 1999)

Using a classical method, cross sections in $A^{q+}+(H,H_2)$ $(q=1,\ldots,8)$ collisions are obtained for impact energy ranges 9 keV amu^{-1}–6.4 MeV amu^{-1} (ionization), –600 KeV amu^{-1} (electron capture). For bare ion impact on H, comparison to experiment and to the results of accurate semiclassical calculations shows that total and partial cross sections, as well as transition probabilities, obtained with the classical trajectory Monte Carlo approach, are more accurate than usually assumed. From the characteristics of the mechanisms, we are led to use our data as estimates for the case of dressed-ion impact at the higher nuclear velocities. We successfully apply a very simple model for H_2 targets, in which the relevant quantities are the charge of the projectile and the vertical ionization potential of the molecule. For practical purposes, we give scaling laws to benchmark (H^+,He^{2+}) cases, and for ionization we relate them, at higher v, to the behavior of the transition probabilities. [S1050-2947(99)05811-4]

PACS number(s): 34.10.+x

I. INTRODUCTION

In recent decades, ionization and electron capture by multicharged ion impact have received (and are still receiving) considerable attention; for ion-atom scattering, see reviews in Refs. [1] and [2]. Of particular theoretical interest is the so-called intermediate energy domain, encompassing the maximum of ionization cross sections. Those processes are also of great practical importance in the physics of impurity control in thermonuclear plasmas [3,4], as well as in astrophysics, ion penetration in solids, and radiation physics. Accordingly, and within a large time span, several experimental groups have undertaken a series of systematic, accurate measurements of capture and ionization cross sections in $A^{q+}+(H,H_2)$ collisions (see, e.g., reviews in Refs. [3,5]). However, some of the measured data are not perfectly suited to the applications. For instance, at the time that the measurements were carried out, the state-of-the-art crossed-beam techniques were often unable to separate data for single-electron processes, such as single ionization or electron transfer, from double processes, such as transfer ionization. Furthermore, the scarcity of theoretical counterparts in a wide energy range, especially for H_2 targets, has resulted in a lack of motivation to redo the previous measurements with more sophisticated coincidence techniques. Moreover, new experiments aim at ''complete'' measurements of differential cross sections involving momentum distributions (see, e.g., Ref. [6]) rather than total ones. The result is that reasonably quantitative information on the latter data at intermediate energies is incomplete.

In recent work [7–10], we concluded that, with some improvements involving the initial conditions and a sufficiently large number of outcomes in the statistics, the classical trajectory Monte Carlo (CTMC) approach [11,12] provides a computationally simple and accurate modeling of collisional processes involving H and H_2 targets, at least with regard to integral cross sections at intermediate v. In this respect, and although a large amount of literature exists on the background of classical methods (e.g., Refs. [11,13–20] and references therein) and ways to improve them including quantal effects (e.g., [21]), it is noteworthy that their accuracy has always turned out to be higher than expected, and the present work shows that they can even be of comparable quality to sophisticated close-coupling treatments including pseudostates. As reasoned in Ref. [22], such a success must be attributed, rather than to the usual high momentum limit of the quantal dynamical treatment [13], to the specific nature of the Coulomb interaction, which leads to additional symmetries and coincidences between quantum-mechanical and statistical classical descriptions. As will be seen, this applies to a wider range of impact energies than often assumed, since some often-quoted defects of the method [15,23,2,3,21] were due to a poor initial choice of the distributions, which is a liability that can be easily remedied (see Refs. [18,24–26] for H and [27] for He targets). One of the purposes here is to ascertain whether the accuracy of the method is high enough to be employed in order to systematize and complete the existing data on $A^{q+}+(H,H_2)$ collisions. Another purpose is to check whether our previous findings on the mechanisms [7,8,10] apply to projectiles other than He^{2+}, before carrying out more detailed studies involving a momentum analysis of the ejected electrons.

With these aims in mind, we have calculated ionization and electron capture cross sections in collisions of bare ions A^{q+} $(q=1,\ldots,8)$ with H,H_2, for a wide range of intermediate impact energies. Furthermore, since our data are smooth functions of q and v, it is easy to obtain (and, to some extent, justify by inspection of the mechanisms) analytical fits that are useful [3] for applications. A very preliminary account of the present data has been given in Ref. [28]. Then, our study of the mechanisms indicated that our data could also be employed to estimate cross sections for partially stripped projectiles, and this point will be explicitly checked by comparison to experiment. For the sake of clarity of the figures, and because of the large amount of literature on the subject, our comparisons will be restricted to what appear to be the most accurate theoretical and experimental data that are available.

The following section summarizes the CTMC approach, which is so well documented [11,12,29,2] that we shall only

give an outline of our procedure, together with a brief summary of the mechanisms. Sections III and IV present our results for H and H_2 targets, respectively, and the scaling fits. Our conclusions are drawn in Sec. V. Atomic units are used throughout unless explicitly stated.

II. CLASSICAL METHOD

A. $A^{q+}+H$ collisions

Our approach for bare ion impact is based on the impact parameter CTMC method [29,2], in which the internuclear vector $\mathbf{R}$ follows linear trajectories $\mathbf{R}=\mathbf{b}+\mathbf{v}t$, with impact parameter $\mathbf{b}$ and velocity $\mathbf{v}$, while the electronic motion is described through an ensemble of trajectories $\{\mathbf{r}_j(t)\}$ that are solutions of the Hamilton equations, so that the corresponding test particle distribution

$$\rho(\mathbf{r},\mathbf{p};v,b,t)=\frac{1}{N}\sum_j \delta(\mathbf{r}-\mathbf{r}_j(t))\delta(\mathbf{p}-\mathbf{p}_j(t)) \qquad (1)$$

satisfies the Liouville equation for the fixed-nuclei electronic Hamiltonian $H_{\rm el}$, with $\mathbf{r}$ and $\mathbf{p}$ the electron position and momentum vector, respectively, with respect to the target (H) nucleus.

Our procedure differs from the usual CTMC algorithm in two respects: (i) use of straight-line trajectories for the nuclei; and (ii) an initial spatial H($1s$) distribution that is close to the quantal one. The approximation (i) does not need to be justified for the impact energy range treated here, because of the large relative nuclear momentum [30–32], and especially in view of the considerable success of the impact parameter semiclassical method to calculate total charge exchange [2] and ionization [1] cross sections. Because of this, integral cross sections obtained from *statistically converged* three-body and impact parameter CTMC calculations can be expected to be identical, provided that the initial distributions are the same. Besides simplifying the computational labor, the present method has the advantage of being more amenable to a study of the mechanisms [7,8], and to a comparison of the transition probabilities with semiclassical counterparts. The modification (ii) is more substantial, and eliminates the inaccuracies of the usual CTMC approach that are due to the choice of an initial microcanonical phase-space distribution:

$$\rho(\mathbf{r},\mathbf{p};v,b,t\to-\infty)=\frac{1}{8\pi^3}\delta\left(\frac{p^2}{2}-\frac{1}{r}+\frac{1}{2}\right). \qquad (2)$$

While this choice has the advantages of stability in time (in the absence of the projectile), and of yielding a momentum density that is identical to the quantal one, its spatial density is too compact, with a cutoff value at $r=2$. To offset this liability, Eichenauer *et al.* [24] proposed the Wigner function as initial distribution, so that both spatial and momentum densities are exact. However, this distribution is unstable, a smoothing procedure is needed to eliminate negative probabilities, and the classical energy $E=p^2/2-1/r$ spreads over a very large domain, including a sizeable portion with $E>0$, where the electron is unbound. Cohen [26] eliminated all these drawbacks with an initial distribution that is a function of energy alone $f(E)$, yielding the exact spatial density, and providing a good approximation of the momentum one. A similar, simpler approach was proposed by Hardie and Olson [25], using a discrete rather than a continuous superposition of microcanonical functions:

$$\rho(\mathbf{r},\mathbf{p};v,b,t\to-\infty)=\sum_{j=1}^{8}\frac{(-2E_j)^{5/2}}{8\pi^3}a_j\delta\left(E_j-\frac{p^2}{2}+\frac{1}{r}\right), \qquad (3)$$

where the energies $E_j=-2/j$ hartree ($j=1,\ldots,8$) were chosen so that the cutoff values $(-E_j)^{-1}$ of the individual spatial densities are in an arithmetic progression; and the weights a_j were calculated so as to achieve good approximations to the spatial and momentum quantal densities, together with $\overline{E}=\Sigma_j a_j E_j=-0.5$ hartree. Because of its simplicity and accuracy [8,9], we have employed this procedure in the present work.

For each nuclear trajectory, and starting from the condition (3), the Hamilton equations were integrated with a variable-step Burlisch-Stoer [33] algorithm. Ionizing and capture trajectories were selected, at the end of the time integration ($t=t_{\rm max}$), by means of the usual energy criterion [17,18,34]. Typically, our statistics involve, for each nuclear path, 30 000 electronic trajectories for $v<1$ a.u. and 20 000 for $v>1$ a.u.; accordingly, the number of trajectories for each v is about an order of magnitude larger than these values; usually, we took $t_{\rm max}=500\,v^{-1}$ a.u., although we found that the same results are often obtained with much smaller values. Convergence of the cross sections was estimated, by varying, in some benchmark cases, the number of trajectories to less than 5% statistical error for ionization and less than 2% error for the capture process. From the asymptotic values of the distribution functions, the ionization $\wp_i$ and capture $\wp_c$ probabilities were calculated by addition over all ionizing or capture test particles:

$$\wp_{i,c}(b,v)=\int d\mathbf{r}\int d\mathbf{p}\rho^{i,c}(\mathbf{r},\mathbf{p};v,b,t_{\rm max}) \qquad (4)$$

and the cross sections were obtained by numerical integration over the impact parameter:

$$\sigma_{i,c}(v)=2\pi\int_0^\infty db\, b\wp_{i,c}(b,v). \qquad (5)$$

An advantage of the classical approach is that it offers a detailed account of the processes in terms of the time evolution of the distributions $\rho(\mathbf{r},\mathbf{p};v,b,t)$. In the course of the present work, we checked that our previous findings [7,8] regarding the *dominant* ionization mechanism are also valid for other projectiles. Neglecting a wealth of details, we now summarize these findings, which are not illustrated for conciseness. For $b\approx 2-3$ a.u., the first step is a polarization of the electron cloud towards the projectile, and the next steps strongly depend on v. When v is larger than that of the maximum of the ionization cross section, the projectile goes so fast that capture is a secondary process, and most polarized electrons are left behind in either an excited, bound state of the target, or, due to the pull from the projectile, they pick up enough energy to ionize. Ionization takes place within a domain of internuclear distances $\Delta R<10$ a.u., and is fol-

lowed by a quasifree expansion [10] of the cloud, yielding the well-known soft electron maximum in the direct ionization mechanism [1]. In the other limit of low v, the drifting process mainly results in electron transfer, which is also a fast process. However, some of the polarized electrons rotate too fast, just miss being captured, and are caught instead by the combined field of the nuclei. Most of this density stays on the saddle region of the potential (although not *at* the saddle point) as the nuclei separate, and, because of a post-collision interaction with the combined nuclear field, their longitudinal momentum density ends up with a maximum at the center of force value [35]. At intermediate v, stronger interactions also take place as a sizeable part of the ionizing cloud collides with either nuclei; the same happens, at low v, for trajectories with $b<2$ a.u.

B. $A^{q+}+H_2$ collisions

Following Ref. [9], our treatment for H_2 targets is based on (i) the sudden approximation, Franck-Condon approach to treat the vibrorotational motion of the diatomic; (ii) an effective Hamiltonian to describe the triatomic system; (iii) the impact parameter CTMC approach to evaluate the single-electron transition probabilities; (iv) the independent-particle model to calculate the two-electron probabilities.

From previous experience in the calculation of total capture cross sections at low energies [36–40], approximation (i) is expected to be very accurate for the energy range treated here. In this formalism, total capture and ionization cross sections are obtained by ignoring vibration and rotation of the diatomic altogether, and keeping, throughout the collision, the distance $\Re_{HH}$ between the two target protons fixed, and equal to the equilibrium value for H_2. The errors can be expected to be even smaller for the reactions with D_2, DT, and T_2 targets, because of the larger reduced masses involved.

Approximation (ii) consists [9,38] of an apparently crude, single-electron model, in which the interaction of the ''active'' electron with the H_2^+ ''core'' is described by means of an effective Coulomb potential $Z_{\rm eff}/r$, where $Z_{\rm eff}=(2U)^{1/2}=1.0995$, with $U=0.60449$ hartree the first vertical ionization potential of H_2 at the equilibrium distance. The model emerges from our finding (Sec. II A) that, for the range of impact parameters that dominate the cross sections, ionization—and to a lesser extent, capture—processes take place relatively far from the target, which is strongly polarized in the way in of the nuclear trajectory. For large distances, ion-molecule interactions depend little upon the relative orientation of the diatomic [37,38] (see also Refs. [41,42]). Even when shorter distances are involved, so that probabilities are strongly anisotropic, one finds [38] that the use of spherically symmetric effective potentials yields good results for the orientation-averaged cross sections, at the impact energies considered here. The approximation can be improved [43,40] by placing the origin of the potential near the nucleus that is closest to the projectile.

Following steps (i) and (ii), we are led to treating the collision between an incident stripped ion and a model single-electron target, and we employ for this purpose the CTMC method [approximation (iii)]. A scaling procedure, explained in Ref. [9], allows the use of the same algorithms to generate the initial distribution when the nuclear charge of the target differs from unity.

Next, total ionization and capture probabilities are calculated [approximation (iv)] in the frame of the independent-particle model (IPM, see, e.g., Refs. [44,45]), assuming two equivalent electrons, as in previous formalisms [46–49]. Explicit checks, using semiclassical methods [50] and non-equivalent as well as equivalent electrons [38], indicate that the IPM is sufficiently accurate for the present purposes, for single ionization or capture processes in the energy domain considered; however, for H_2 targets, it fails [9] for double-electron processes, as predicted in Ref. [49]; for conflicting evidence on this point for the much simpler case of collisions with He targets at intermediate v, see, e.g., Refs. [51] and [52]. In the present work, this limitation of the method is only an inconvenience in the comparison with measured data including contributions from double processes.

In the frame of the IPM, one obtains the two-electron probabilities from the single-electron counterparts $\wp_{c,i}$ and $\wp_e(b,v)=1-\wp_c(b,v)-\wp_i(b,v)$, through the following standard expressions:

$$\text{single electron capture:}\quad P_{\rm sc}=2\wp_c\wp_e, \tag{6}$$

$$\text{single electron ionization:}\quad P_{\rm si}=2\wp_i\wp_e, \tag{7}$$

$$\text{transfer ionization:}\quad P_{\rm ti}=\wp_i\wp_c, \tag{8}$$

$$\text{double capture:}\quad P_{\rm dc}=\wp_c^2, \tag{9}$$

$$\text{double ionization:}\quad P_{\rm di}=\wp_i^2. \tag{10}$$

When the center of the effective potential is at the midpoint of the H-H axis, the probabilities $P(b,v)$ only depend on the modulus of the impact parameter **b** and relative velocity **v** vectors, so that integration over the former yields the corresponding cross section:

$$\sigma(v)=2\pi\int P(b,v)b\,db. \tag{11}$$

On the other hand, when the center can be at a H nucleus, the probabilities P(**b**,**v**) also depend upon the orientation of **b**,**v** with respect to the diatomic internuclear vector $\Re_{HH}$. Then, an averaging over the orientation of **v** and an integration over **b** (with **b**$\perp$**v**) yield the corresponding cross sections $\overline{\sigma}_{\rm sc}(v),\overline{\sigma}_{\rm si}(v),\overline{\sigma}_{\rm ti}(v),\overline{\sigma}_{\rm dc}(v),\overline{\sigma}_{\rm di}(v)$. This averaging was performed in Ref. [9] in an approximate way that we briefly summarize. Following the computational scheme method of Ref. [36], the cross section is given as the result of quadratures of P(**b**,**v**) over **v** directions and impact parameters **b**, ascribing equal weights to trajectories parallel to $\Re_{HH}$, and to the two sets of trajectories perpendicular to this axis. The present work adopts the same procedure, except that we take the origin of the potential at the center of the molecule for the parallel trajectories and for those perpendicular ones that are equidistant to both H nuclei. For the other perpendicular trajectories, we take the origin at the H nucleus that is closest to the projectile. Under a distant collision hypothesis, we then neglect contributions from trajectories with $b<\Re_{HH}/2$, thus obtaining the following simple expression:

TABLE I. (a) Calculated ionization cross section (in units of 10^{-16} cm^2) for $A^{q+}+\mathrm{H}(1s)$ collisions, as a function of the nuclear velocity (in atomic units). The data for which our calculations are thought to be inaccurate are not given. (b) Calculated electron capture cross section (in units of 10^{-16} cm^2) for $A^{q+}+\mathrm{H}(1s)$ collisions, as a function of the nuclear velocity (in atomic units). The data for which our calculations are thought to be inaccurate are not given.

v (a.u.)	H^+	He^{2+}	Li^{3+}	Be^{4+}	B^{5+}	C^{6+}	N^{7+}	O^{8+}
				(a)				
0.6	0.263	0.172	0.139	0.096				
0.8	0.584	0.482	0.381	0.300	0.235	0.176	0.180	0.163
1.0	1.293	1.661	1.500	1.347	1.270	1.097	0.956	0.823
2.0	1.463	4.858	8.977	13.142	17.592	21.674	25.506	29.204
3.0	0.737	2.763	5.781	9.565	13.862	18.578	23.569	28.754
5.0	0.242	0.962	2.139	3.688	5.724	8.077	10.760	13.754
8.0	0.102	0.417	0.911	1.583	2.488	3.526	4.779	6.175
10.0	0.069	0.285	0.633	1.102	1.699	2.437	3.292	4.276
12.0	0.046	0.206	0.451	0.807	1.238	1.774	2.404	3.126
14.0	0.036	0.148	0.335	0.585	0.918	1.314	1.791	2.308
16.0	0.025	0.106	0.247	0.443	0.670	1.001	1.367	1.779
				(b)				
0.6	4.870	13.054	20.925	29.195				
0.8	4.629	12.713	20.537	28.742	36.968	45.189	53.430	61.365
1.0	3.065	4.213	16.865	24.426	32.036	39.837	47.669	55.418
2.0	0.151	0.745	1.807	3.278	5.130	7.459	10.185	13.250
3.0	0.007	0.047	0.128	0.247	0.410	0.613	0.866	1.619
5.0			0.001	0.003	0.005	0.007	0.013	0.020

$$\overline{\sigma}(v)=2\pi\int_0^\infty db(b+\Re_{\mathrm{HH}}/6)P(b,v). \tag{12}$$

This yields slightly more reasonable ''error bars'' $\sigma-\overline{\sigma}$, estimating the effects of the anisotropy of the $A^{q+}+H_2$ interaction, than the procedure adopted in Ref. [9].

III. RESULTS AND DISCUSSION

A. $A^{q+}+\mathrm{H}(1s)$ collisions

1. Cross sections for bare projectiles

In Table I we present some values of our calculated cross sections for single ionization $\sigma_i(v)$ (a) and electron capture $\sigma_c(v)$ (b) in collisions involving stripped ions A^{q+} with charge $q=1,\ldots,8$. In Figs. 1 and 2, we show the general good accord between these data and the results of other accurate calculations and experiments. For the sake of clarity, we omit the (small) estimates of the experimental error bars, and we do not show the improvement with respect to microcanonical CTMC calculations.

The most sensitive test on the accuracy of our calculations refers to H^+ projectiles, because a classical approach cannot describe [21] the resonant charge-transfer process $H^+ + \mathrm{H}(1s)\rightarrow \mathrm{H}(1s)+H^+$, which competes with ionization at low energies. It is therefore gratifying that in Fig. 1 our values for σ_i are in such good accord with those of very accurate atomic (Toshima [53,54]) and molecular (Errea *et al.* [55]) close-coupling treatments, in a wide range of energies. From this accord, and since error bars in the measurements of Shah *et al.* [56,57] are tiny, we are led to agree with Toshima [54] on a possible error in the normalization (to Ref. [58]) of those measurements. For the sake of clarity, we do not show the small differences with the results of Hardie and Olson [25] and Cohen [26], which are due [9] to our improved statistics.

With respect to charge exchange by H^+ impact, we observe in Fig. 2 a good degree of accord with the measurements of McClure [59], for $v>1$ a.u. At lower v, our data lie below the experiment, unlike the semiclassical results of Errea *et al.* [55]. This is as expected, since, as mentioned above, a classical approach cannot describe the resonant charge transfer. Comparison with Hardie and Olson [25] and Cohen [26] follows as for ionization, and is not shown; in particular, we checked that our capture probabilities are in even better agreement with the corresponding (oscillating) data of the latter author than is the case of the corresponding cross sections.

As the projectile charge $q>1$ increases, we obtain an improving accord of our values for ionization, with the semiclassical results and the measurements. This is already apparent in Fig. 2 for the benchmark $He^{2+}+\mathrm{H}(1s)$ reaction, for which we compare well to experiment (Shah *et al.* [60,61]) as well as to semiclassical calculations (Winter [62,63], Toshima [53], Kuang and Lin [64], and Errea *et al.* [55]), except that at low v the results of Winter overestimate σ_i. Similar comments apply to Li^{3+} projectiles. For $1<v<3$ a.u. we closely agree with the converged, close-coupling calculations of Toshima [53], while the accord with the continuous distorted wave (CDW) data of Crothers *et al.* [65,66] is only reasonable at energies that are too low for a perturbative approach.

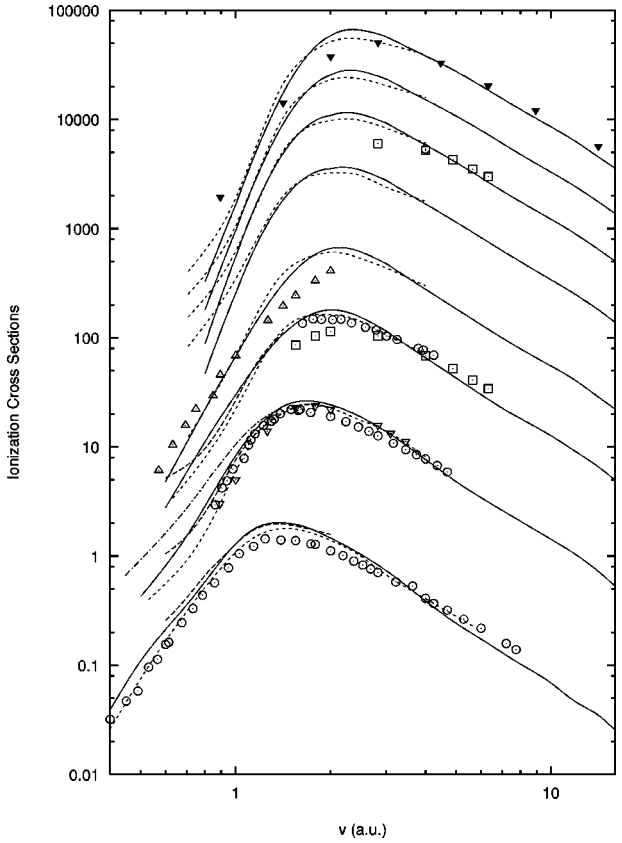

FIG. 1. Ionization cross section for $A^{q+}+\mathrm{H}(1s)$ collisions, as a function of the nuclear velocity (in atomic units). (——) are present calculations. The data are given in units of 10^{-16} cm^2 and scaled as follows. For H^+ projectiles: (⊙) measurements from Shah *et al.* [56,57]; theoretical results from (----) Toshima [54], (- - -) Errea *et al.* [55]. For He^{2+} projectiles (data×5): (⊙) measurements of Shah *et al.* [60,61,56]; theoretical results from (----) Toshima [53], (- - -) Errea *et al.* [55], (— · — · — · —) Winter [62,63], (▽) Kuang and Lin [64]. For Li^{3+} projectiles (data×20): (⊙) measurements of Shah *et al.* [94,109]; theoretical results from (----) Toshima [53], (- - -) Errea *et al.* [55]; (□) Crothers and McCann [66]. For Be^{4+} projectiles (data×50): (△) theoretical results from (----) Toshima [53], Schultz *et al.* [106]. For B^{5+} projectiles (data×200): theoretical results from (----) Toshima [53]. For C^{6+} projectiles (data ×500): (⊙) measurements from Goffe *et al.* [71,96]; theoretical results from (----) Toshima [53], (□) Crothers [65]. For N^{7+} projectiles (data×1000), theoretical results from (----) Toshima [53]. For O^{8+} projectiles (data×2000), theoretical results from (----) Toshima [53], (full triangle down) recommended data from Janev *et al.* [111].

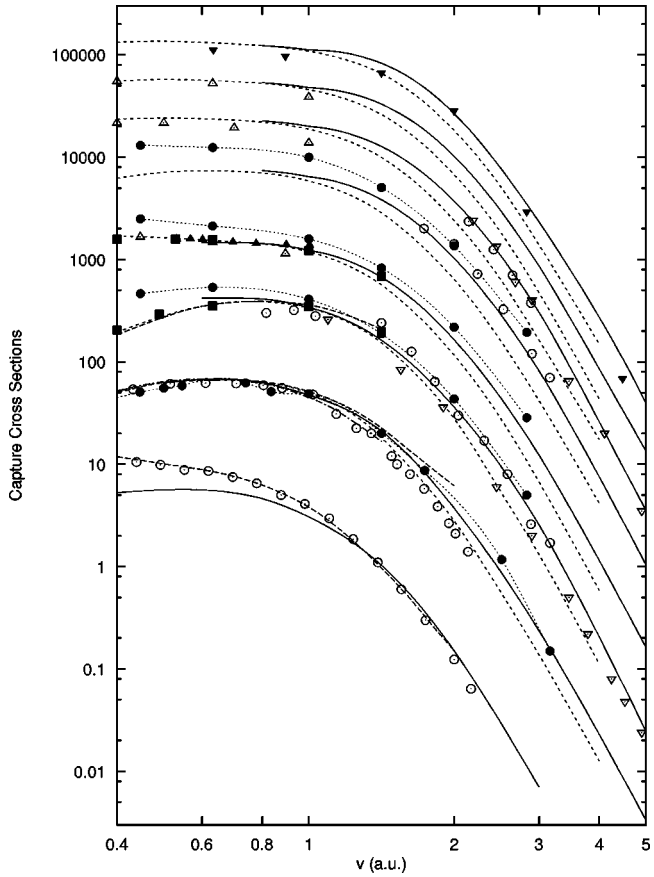

FIG. 2. Electron capture cross section for $A^{q+}+\mathrm{H}(1s)$ collisions, as a function of the nuclear velocity (in atomic units). (——) are present calculations. The data are given in units of 10^{-16} cm^2 and scaled as follows. For H^+ projectiles: (⊙) measurements of McClure [59]; theoretical results from (— — —) Errea *et al.* [55]. For He^{2+} projectiles (data×5): (⊙) measurements of Shah *et al.* [56]; theoretical results from (----) Toshima [53], (- - -) Errea *et al.* [55], (— · — · — · —) Winter [62,63], (· · ● · ·) Bransden *et al.* [67]. For Li^{3+} projectiles (data×20): (⊙) measurements of Shah *et al.* [57]; theoretical results from (----) Toshima [53], (- - -) Errea *et al.* [55], (▽) Gravielle and Miraglia [68], (· · ● · ·) Bransden *et al.* [67], (full box) Lüdde and Dreizler [69]. For Be^{4+} projectiles (data×50): theoretical results from (----) Toshima [53], (· · ● · ·) Bransden *et al.* [67], (full box) Lüdde and Dreizler [69], (△) Fritsch and Lin [103], (full triangle up) Wada and Murai [70]. For B^{5+} projectiles (data×200): (⊙) measurements from Shah *et al.* [71]; theoretical results from (----) Toshima [53], (· · ● · ·) Bransden *et al.* [67]. For C^{6+} projectiles (data×500): (⊙) measurements from Shah *et al.* [71]; theoretical results from (----) Toshima [53], (▽) Gravielle and Miraglia [68], (△) Fritsch and Lin [103]. For N^{7+} projectiles (data×1000): theoretical results from (----) Toshima [53], (△) Fritsch and Lin [103]. O^{8+} (×2000): theoretical results from (----) Toshima [53], (full triangle down) recommended data from Janev *et al.* [111].

For electron capture (Fig. 2), the comparisons are similar to those for ionization, except that as v increases our results are systematically higher than those of Toshima [53], which is a feature that we are unable to explain. For He^{2+} projectiles, we obtain closer results to Bransden *et al.* [67], who, like Toshima, use an atomic expansion, while the data from the latter author agree better with experiment. For $Li^{3+}+\mathrm{H}(1s)$, our data coincide with experiment and with Bransden *et al.* [67], while those of Ref. [53] are smaller, and agree with the CDW results from Gavrielle and Miraglia [68]. At low v, we reach a good accord with experiment and with the close-coupling calculations of Lüdde *et al.* [69], who use a dynamical basis, while Bransden *et al.* [67] appear to overestimate σ_c, which is a discrepancy that increases with q. For $Be^{4+}+\mathrm{H}$, we compare well to the close-coupling results of Wada and Murai [70] carried out at low v, and for $C^{6+}+\mathrm{H}$, to both experiment [71] and Ref. [68], while Ref. [53] appears to underestimate σ_c.

2. Accuracy of probabilities and partial cross sections

We illustrate here the accuracy of our data for the transition probabilities and partial cross sections. For conciseness, only a limited amount of these data will be presented.

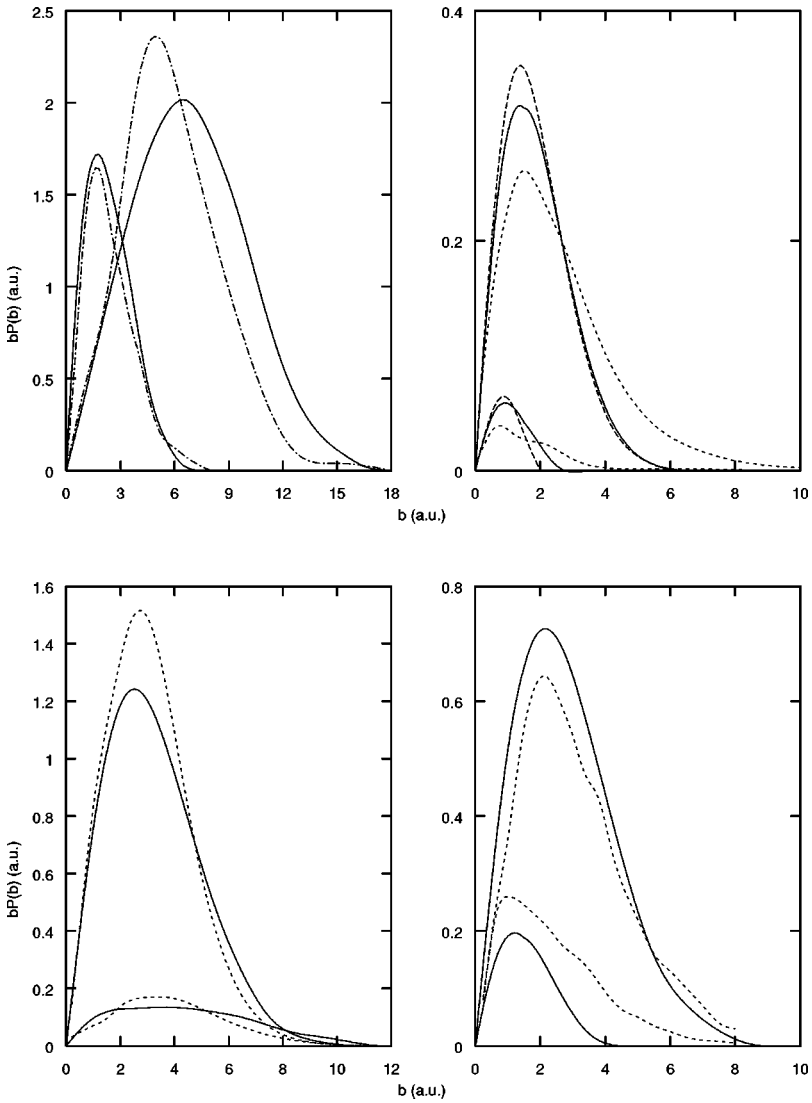

FIG. 3. Ionization and capture probabilities $P(b)$ times the impact parameter b, as functions of b (in a.u.), for $A^{q+}+\mathrm{H}(1s)$ collisions. Present results (——). O^{8+} and H^+: (— . — . — . —) ionization results from Toshima for O^{8+} at $v=2$ a.u. [53] and for $H^+(\times 5)$ (compact one) at $v=1.4142$ a.u. [54] (top left). H^+ for $v=2$ a.u.: (----) data from Errea *et al.* [55]; (— — —) data from Eichenauer *et al.* [24] [$bP_i(b)$ is the higher one] (top right). He^{2+} for $v=1$ a.u.: (----) data from Errea *et al.* [55] [$bP_c(b)$ is the higher one] (bottom left). He^{2+} for $v=2$ a.u.: (----) data from Errea *et al.* [55] [$bP_i(b)$ is the higher one] (bottom right).

We display in Figs. 3(a)–3(d) our values for $b\wp_c(b)$ with the results of the molecular calculation from Errea *et al.* [55] for collisions with H^+ and He^{2+} projectiles, and with data from Toshima [53,54] for O^{8+} and H^+ impact. To our knowledge, this is the first direct comparison between classical and semiclassical transition probabilities, and shows that the good accord between the cross sections is not coincidental.

With respect to partial cross sections, we present in Table II the results of applying the ''boxing'' procedure of Becker and McKeller [72] (derived for a microcanonical distribution, see also Refs. [73–75]) to obtain, from our data, capture cross sections for collisions with He^{2+}, Li^{3+}, C^{6+}, and O^{8+} projectiles, and we compare these results to those of the close-coupling calculations from Harel *et al.* [76]. An overall agreement holds, although the accord is better, in general, for total than for partial cross sections. We attribute the discrepancies involving the $n=5,6$ energy levels of O^{7+} to saturation effects in the close-coupling calculations, due to back-coupling [77], rather than to the classical method [75]. On the other hand, for the lower energy levels, the fault probably lies with the classical data, and a deficiency in the ''boxing'' procedure of Becker and McKeller is a likely explanation.

3. Scaling rules

The usefulness of analytical scaling relations for ionization [60,23,78,3] and capture [2,78,3] cross sections, as functions of the projectile charge and nuclear velocity, is very well known. In this respect, it is worth noting that, although classical methods have the advantage to obey exact scaling rules [11,12,25,18,79,19], these are not useful here, because they involve changing the target initial energy. Therefore, our rules are, to a large extent, empirical, and based on explicit calculations for A^{q+} projectile impact, for $q=1,\ldots,8$ and different velocities. Nevertheless, they yield, for ionization, some additional information on the mechanisms.

For instance, a relevant issue is the often-quoted [15,26,3,2] property of the usual CTMC approach, which yields an inaccurate energy dependence $\sigma_i \propto E^{-1}$, at large v, rather than the Bethe-Born limit behavior (Mott and Massey [80], Gillespie [23], Willis *et al.* [16]):

$$\sigma_i^{\mathrm{Bethe}}(v)=\mathcal{A}q^2[\ln \mathcal{C}^{1/2}+\ln(v/\overline{v})]/(\overline{v}v)^2. \qquad (13)$$

However, when using an initial distribution that yields accurate spatial and momentum densities, the results are more

TABLE II. Partial electron capture cross sections to H(n) in units of 10^{-16} cm^2 for different A^{q+} projectiles ($A^{q+}=He^{2+}$, Li^{3+}, C^{6+}, and O^{8+}) at $v=1$ a.u. compared to the corresponding results of close-coupling molecular calculations [76]. Total capture cross section σ_c is also included. We do not include data that are less than 10^{-19} cm^2 and those from [76] that have not been calculated due to basis limitations.

	He^{2+}		Li^{3+}		C^{6+}		O^{8+}	
n	CTMC	MOCC	CTMC	MOCC	CTMC	MOCC	CTMC	MOCC
1	0.63	0.15	0.06					
2	5.32	7.97	4.46	6.07	0.19		0.04	
3	2.02	1.92	6.9	8.55	3.86	3.55	0.94	
4	0.69	0.68	2.8	2.27	10.21	18.8	5.95	7.53
5	0.30		1.11	1.2	11.14	12.3	12.01	23.9
6	0.17		0.54		7.09	5.42	13.78	19.56
7	0.09		0.29		3.36		10.06	7.84
8	0.06		0.18		1.45		5.82	
9	0.04		0.11		0.75		2.82	
10	0.03		0.09		0.42		1.25	
σ_c	9.49	10.7	16.86	18.1	39.84	40.1	55.4	58.8

compatible with the Bethe-Born law than with the E^{-1} dependence [9]. We show this in Table III, taking in Eq. (13) the values $\mathcal{C}=84.241$ from Willis *et al.* [16]; $\overline{v}=1$ a.u. as the average orbital velocity of the electron in its initial state; and $\mathcal{A}=1.46\times10^{-16}$ cm^2, obtained in Ref. [9] by fitting the data for H^+ projectiles. We also include in the table the result of assuming an $\sigma_i \propto E^{-1}$ law. We see that $\sigma_i^{\text{theor}} \simeq \sigma_i^{\text{Bethe}}$, although the degree of approximation worsens when q increases, probably because $\mathcal{A}$ has been fitted to our calculated σ_i for H^+ impact, which is less accurate than for other projectiles.

It should be noticed from Table III that for heavy projectiles the Born-type q^2 variation of our calculated σ_i holds even when the standard condition [81,82,1] $v \gg q$ for the Born perturbation method is not fulfilled. The justification must obviously lie with the behavior of the ionization probabilities $\wp_i(v,b,q)$, for the range of impact parameters that determine the cross section (rather than for all b). We note that previous work on this point using semiclassical theory is not useful: although a q^2 dependence of $\wp_i(v,b,q)$ for fixed v,b is predicted [1], the reference quoted is from Hansteen [82], who gives as a necessary condition that the projectile charge be much larger than that of the target nucleus, which is not the case of our systems. We were thus led to study the q dependence of the classical ionization process. At low v, we found that no simple overall scaling rule exists for $\wp_i(v,b,q)$, because each of the mechanisms (saddle-point, hard encounters with projectile and/or target nucleus) that are at work [7,9] vary with v,b,q in a different way. On the other hand, for $v>v_{\max}$ larger than those of the maximum of $\sigma_i(v)$, these probabilities are dominated by a single (direct) mechanism, and we found two approximate laws, both of them leading to $\sigma_i \propto q^2$.

First, for fixed $v>v_{\max}$, the number of ionized electrons in the statistics [hence, the value of $\wp_i(v,b,q)$] grows quadratically with q for the impact parameters b that determine the cross sections [i.e., those close to the maximum of $bP(b)$]; while for lower b, we observe the so-called saturation effects [1] when the q^2 scaling would lead to probabilities close to, or larger than, unity. Second, we also found a relation that holds for a slightly larger b domain: for fixed values of v,b', where $b'=bq^{-1/2}$, $\wp_i(v,b,q)$ turns out to be proportional to q, to a good approximation. The use of a $bq^{-1/2}$ scaling bears some relation to a distant collision hypothesis to estimate the impact parameter range where ionization is dominant, as introduced by Voitkiv and Pazdzerky [83] (see also Rodríguez and Falcón [79], and, for excitation, Fritsch and Schartner [84] and Rodríguez and Miraglia [85]). Nevertheless, we note that, unlike these works, our scaling is for fixed v and yields a probability that is linear in q.

From our findings, and taking Ref. [23] and Eq. (13) as guidelines, we have obtained a simple fit of our calculated ionization cross sections to the results for H^+ projectiles:

$$\sigma_i^{\text{scaled}}(q,v)=\sigma_i(1,v)q^{2[1-e^{-1.4(v-0.76-0.04q)}]}. \tag{14}$$

For $v \geqslant 1$ a.u., the maximum absolute error of this law with respect to our calculated values of σ_i is about $0.1q^2$, for $v \simeq v_{\max}$, in the peak region of the cross sections.

For electron capture, our procedure is similar to previous work (e.g., Ref. [3]), except that, since our method is less accurate at low v for $H^+ + H$, as explained in the preceding section, it is more suitable to scale our data to σ_i for He^{2+} projectiles, and we obtain

$$\sigma_c^{\text{scaled}}(q,v')=\sigma_c(2,v)\left(\frac{q}{2}\right)^{1.15} \tag{15}$$

with $v'=v(q/2)^{0.175}$. It predicts a quasilinear q dependence, which is usually obtained in the low-energy regime (Janev and Winter [78]). At intermediate v, it is similar to those of Ryufuku *et al.* [86–88], and differs from Refs. [71,89,78,3] in that we do not obtain the same q^3 dependence that holds at higher v [89,3]. Regarding the velocity variation, we find a similar behavior to other authors (Janev *et al.* [90], Ryufuku *et al.* [86–88]). Because of the rapidly decreasing character of the capture cross sections, it is difficult to give estimates of the accuracy of Eq. (15), since the absolute errors diminish like the cross sections, and the relative errors diverge. As

TABLE III. Large-v behavior of our calculated ionization cross sections $\sigma_i^{\text{theor}}(v)$ (in units of 10^{-16} cm^2) for $A^{q+}+\text{H}(1s)$ collisions, as a function of the nuclear velocity v (in atomic units). We compare with the values obtained from the Bethe-Born expression $\sigma_i^{\text{Bethe}}(v)$ of Eq. (13), with $\mathcal{C}=84.241$ [16], $\overline{v}=1$ a.u., and $\mathcal{A}=1.46\times10^{-16}$ cm^2 [9]; together with the values of $\sigma_i^{E^{-1}}=(25/v^2)\sigma_i^{\text{theor}}(v=5)$, obtained by assuming a $\sigma_i \propto E^{-1}$ law.

	H^+			He^{2+}		Li^{3+}		Be^{4+}	
v (a.u.)	σ_i^{theor}	σ_i^{Bethe}	σ_i^{E-1}	σ_i^{theor}	σ_i^{Bethe}	σ_i^{theor}	σ_i^{Bethe}	σ_i^{theor}	σ_i^{Bethe}
5.0	0.242	0.223		0.962	0.893	2.139	2.010	3.688	3.574
8.0	0.102	0.099	0.094	0.417	0.392	0.911	0.885	1.583	1.567
10.0	0.069	0.066	0.061	0.285	0.264	0.633	0.594	1.102	1.056
16.0	0.025	0.028	0.023	0.106	0.114	0.247	0.256	0.443	0.455

	B^{5+}		C^{6+}		N^{7+}		O^{8+}	
v (a.u.)	σ_i^{theor}	σ_i^{Bethe}	σ_i^{theor}	σ_i^{Bethe}	σ_i^{theor}	σ_i^{Bethe}	σ_i^{theor}	σ_i^{Bethe}
5.0	5.724	5.575	8.077	8.042	10.760	10.945	13.754	14.236
8.0	2.488	2.475	3.526	3.527	4.779	4.800	6.175	6.270
10.0	1.699	1.650	2.437	2.376	3.292	3.234	4.276	4.223
16.0	0.670	0.700	1.001	1.025	1.367	1.395	1.779	1.822

an indication, the largest absolute error with respect to our calculated values of σ_c is, at low v, of the order $(q/2)^{1.15}$ (for $q=5$).

4. Application of our data to dressed projectiles

In their paper on dressed-ion A^{q+} impact on H($1s$), Shah *et al.* [91] pointed out that ionization cross sections are roughly independent of the number of electrons of the projectile, for a given total charge q; an exception arises for $q=2$ at low v, where the values of σ_i for the dressed projectiles are much larger than for He^{2+}. It is useful to check whether these findings hold for other systems, since one could then use our data, or Eq. (14), for collisions that have not been treated experimentally, such as for Be^{q+} ($q=2,3$) projectiles, or for impact by partially stripped ions A^{q+} with $q>5$. A similar application has been proposed by Gillespie [23] for $q>Z/2$.

It is interesting that such an application is, to some extent, borne out by our study of the mechanisms, since both the initial polarization of the H($1s$) cloud and the pull from the projectile (either in direct ionization or in the saddle-point process) depend critically on the net ionic charge q, besides that of the target nucleus. In addition, in the limit of high $v \gg v_{\max}$, the assumption would also agree with the conclusions from the first-order Born approximation, as first developed by Bates and Griffing [58] (see also Briggs and Taulbjerg [92] and McGuire *et al.* [93]), where, for soft ionizing electrons, the role of the projectile core is to screen the nuclear charge; however, see below. We note that our study of core effects differs from most others (see references in Stolterfoht *et al.* [1]) in that we keep q fixed and vary the nuclear charge Z.

We compare in Fig. 4 our ionization data for bare projectiles to the measurements from Goffe *et al.* [71] and Shah *et al.* [94,91,95,96,61,56,57] for partially stripped projectiles colliding with H($1s$). We see that the assumption of Z invariance for fixed q holds, for $q>1$ and $v \geqslant v_{\max}$ a.u.—hence, in a wider q domain than suggested in Ref. [23], see Ref. [3]—where our accord with experiment is nearly as good for bare and dressed projectiles. It holds, in particular for impact energies that are much too low for the first Born approximation to be valid. In fact, this approximation may turn out to be irrelevant to this topic, since there is an indication that the agreement worsens as v increases, because cross sections are dominated by close encounters for which core electrons play a more direct role [93].

The main discrepancy (already noticed by Shah *et al.* [91] for $q=2$) between the data for bare and partially stripped projectiles appears for $v<v_{\max}$. This point is worth commenting upon, as it may lead to detailed investigations using correlated wave functions or pseudopotentials [97]. Nevertheless, we must first rule out the possibility of additional contributions to σ_i in the measurements of the Belfast group. For instance, since the ions arising from ionization processes were selectively recorded by counting them in coincidence with the electrons from the same events, we can rule out ionization of the core electrons (the projectile then acting as a target). Furthermore, the contributions to the H^+-e^- coincidence signal arising from dissociative ionization of H_2 molecules and from residual gases (mainly H_2O) in the vacuum chamber led to an extra contribution to the signal from H_2 molecules [91], which is rather large at the lower impact energies, but which was accurately taken into account in the experiments. In addition, any such contribution is the same for both dressed and bare projectiles, so it would not explain the difference between the corresponding cross sections.

We thus conclude that, at low impact energies, the core of the impinging ion must play a direct role in the mechanism. One possibility is that, since screening of the projectile charge by the core is incomplete, the relevant quantity would be the effective charge, Z_{eff}, felt by the target electron as it approaches the projectile nucleus, rather than the total charge of the ion, q. To estimate the importance of this effect, we can take $Z_{\text{eff}}=n\sqrt{2U_{\text{ion}}}$, where U_{ion} is the ionization potential of $A^{(q-1)+}$ and n is the outermost shell of the core. We then note that either use of Eq. (14) or inspection of Fig. 1 shows that substituting $q \to Z_{\text{eff}}$ decreases σ_i in the threshold

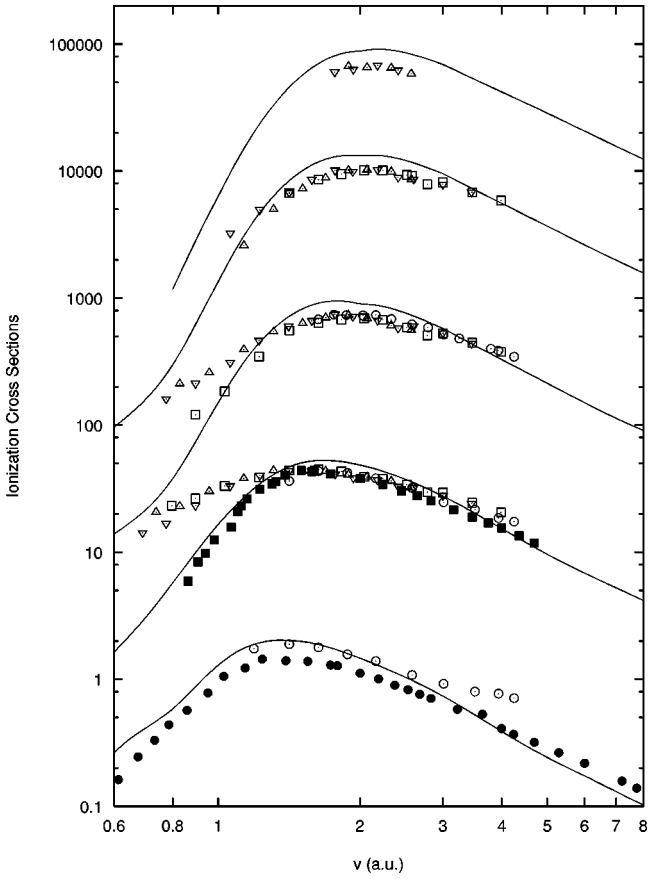

FIG. 4. Comparison of the present results (——) for the single ionization cross section of $A^{q+}+\mathrm{H}(1s)$ collisions, with A^{q+} a bare ion, with experimental data for stripped and dressed A^{q+} projectiles. Theoretical results are the same as in Fig. 1, except that the scaling is different, and are given as functions of the nuclear velocity (in atomic units). The data are given in units of 10^{-16} cm^2 and scaled as follows. $q=1$: data from Shah *et al.* for H^+ [56,57] (●) and Li^+ [57] (⊙). $q=2(\times 10)$: data from Shah *et al.* for He^{2+} [60,61,56] (full box), Li^{2+} [95] (⊙), C^{2+} [91,96] (□), N^{2+} [91] (△), and O^{2+} [91] (▽). $q=3(\times 100)$: data from Shah *et al.* for Li^{3+} [95] (⊙), C^{3+} [91,96] (□), N^{3+} [91] (△), and O^{3+} [91] (▽). $q=4(\times 1000)$: data from Shah *et al.* for C^{4+} [91,96] (□), N^{4+} [91] (△), and O^{4+} [91] (▽). $q=5(\times 5000)$: data from Shah *et al.* [91] for N^{5+} (△) and O^{5+} (▽).

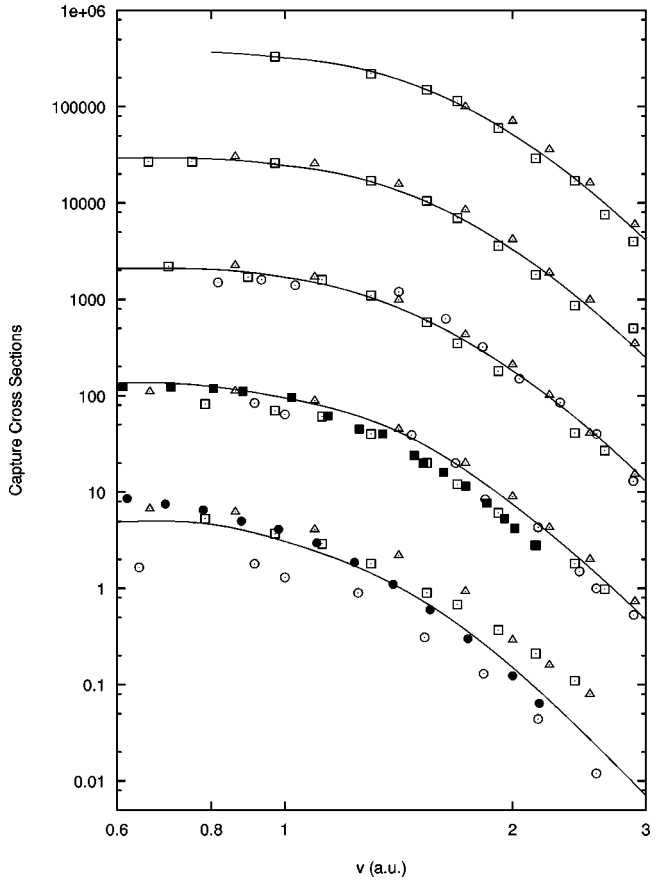

FIG. 5. Comparison of the present results (——) for the electron capture cross section of $A^{q+}+\mathrm{H}(1s)$ collisions, with A^{q+} a bare ion, with experimental data for stripped and dressed A^{q+} projectiles. Theoretical results are the same as in Fig. 1, except that the scaling is different, and are given as functions of the nuclear velocity (in atomic units). The data are given in units of 10^{-16} cm^2 and scaled as follows. $q=1$: data from McClure for H^+ [59] (●), data from Shah *et al.* for Li^+ [94] (⊙), B^+ [71] (△), and C^+ [71] (□). $q=2(\times 10)$: data from Shah *et al.* for He^{2+} [94] (full box), Li^{2+} [94] (⊙), B^{2+} [71] (△), and C^{2+} [71] (□). $q=3(\times 100)$: data from Shah *et al.* for Li^{3+} [94] (⊙), B^{3+} [71] (△), and C^{3+} [71] (□). $q=4(\times 1000)$: data from Shah *et al.* for B^{4+} [71] (△) and C^{4+} [71] (□). $q=5(\times 10\,000)$: data from Shah *et al.* for B^{5+} [71] (△) and C^{5+} [71] (□).

region. Hence, a more sophisticated choice of $Z_{\mathrm{eff}}(r)$ depending upon the electronic coordinate would also yield smaller results, so that penetration effects cannot explain the larger values of σ_i in Fig. 4 for the dressed projectiles.

Next, inspection of the arrow diagrams illustrated in Ref. [8] to describe the ionization process shows that the only modification of the mechanism that is likely to yield such an increase of the cross section at threshold must involve the saddle-point process. More precisely, two-center dielectronic processes [58,92,93,98–100], when the saddle region overlaps the inner shell of the dressed ions, could enhance the probability of single ionization. Such an effect would be smaller for dressed ions with an $n=1$ inner shell (i.e., with a smaller spatial extent). However, since we have no experimental data, nor theoretical means, to check this prediction, our reasoning remains speculative, and the detailed nature of the dielectronic processes is an open question.

Our capture data can also be applied to partially stripped ion impact, as shown in Fig. 5. As may be expected, the $q=1$ case is special, such that ignoring the core structure is too naive. For $q=2$, the accord between bare and dressed-ion data is reasonable, and improves with increasing q. This may be easily explained by comparing the range Δb of impact parameters determining σ_c to the sum Δr of the sizes of target and projectile electron clouds [using, e.g., for the latter the value $\sqrt{\langle r^2\rangle}=(n/2Z)\sqrt{5n^2+1}$, where n is the principal quantum number of the outermost shell and Z is the net charge felt by the electrons of this shell]. We do not show this comparison for conciseness, and only comment that for Li^+, B^+, and C^+ projectiles Δr is of the order of Δb and is smaller for the other systems treated. We have checked that the agreement is not improved when one substitutes in Eq. (15) the net charge q by a partially screened one. Hence, we conclude that the influence of the core in the capture process

TABLE IV. (a) Calculated single ionization cross section [$\overline{\sigma}(v)$ of Eq. (12), and in units of 10^{-16} cm^2] for $A^{q+}+H_2$ collisions, as a function of the nuclear velocity (in atomic units). The data for which our calculations are thought to be inaccurate are not given. (b) Calculated single electron capture cross section [$\overline{\sigma}(v)$ of Eq. (12), and in units of 10^{-16} cm^2] for $A^{q+}+H_2$ collisions, as a function of the nuclear velocity (in atomic units). The data for which our calculations are thought to be inaccurate are not given.

v (a.u.)	H^+	He^{2+}	Li^{3+}	Be^{4+}	B^{5+}	C^{6+}	N^{7+}	O^{8+}
				(a)				
0.6	0.235	0.112		0.019				
0.8	0.697	0.405	0.279	0.237	0.164	0.138		
1.0	1.095	1.023	0.877	0.814	0.773	0.684	0.642	0.538
2.0	2.069	5.511	9.036	12.502	15.724	18.893	21.735	24.304
3.0	1.232	3.732	6.549	9.741	13.191	16.697	20.511	24.295
5.0	0.301	1.615	3.119	4.786	6.677	8.750	10.978	13.410
8.0	0.199	0.725	1.486	2.413	3.454	4.613	5.8485	7.163
10.0	0.127	0.488	1.040	1.699	2.475	3.354	4.293	5.282
12.0	0.096	0.368	0.772	1.289	1.874	2.514	3.241	4.044
14.0	0.070	0.292	0.615	1.019	1.487	2.018	2.569	3.212
16.0	0.058	0.214	0.491	0.814	1.195	1.626	2.115	2.615
				(b)				
0.6	6.451	13.214						
0.8	5.932	12.286	18.396	22.872	29.422	34.684		
1.0	4.608	10.557	16.251	21.724	27.234	32.679	38.133	43.432
2.0	0.237	0.799	1.491	2.503	3.812	5.210	6.937	8.910
3.0	0.0184	0.008	0.133	0.184	0.253	0.341	0.444	0.563
5.0		0.002	0.004	0.004	0.004	0.004	0.005	0.007

is not that of a simple penetration effect, and must also involve local electron-electron interactions.

B. $A^{q+}+H_2$ collisions

1. Cross sections for bare projectiles

In Table IV we present some values of our calculated orientation-averaged cross sections for single ionization $\overline{\sigma}_{si}$ (a) and capture $\overline{\sigma}_{sc}$ (b) in collisions involving stripped ions with charge $q=1,\ldots,8$. For H^+ projectiles, the present data are slightly more accurate than those of Ref. [9]. Comparison of these data with those of Table I bears on the question of whether the H_2 target is equivalent to two H atoms, and shows that our previous conclusions [9] remain unchanged for $q>1$. Specifically, for ionization, we obtain, for $v<v_{max}$, a rough agreement of the cross sections for H and H_2 targets, due to a compensation effect: a lowering of the ionization probability $\wp_i$ for the ''active'' electron of H_2 with respect to that of H and an increase when $\wp_i$ is employed in the expression (7) to obtain P_{si}, because $\wp_e>0.5$. When $v \gg v_{max}$, we have $\wp_e \approx 1$, and accordingly the ionization data for the molecular target roughly tend to twice the atomic values, as assumed in previous scalings [101,102]. A similar behavior is found for the electron-capture cross sections.

In Figs. 6 (ionization) and 7 (capture) we compare our results for H_2 targets with those of other calculations (Fritsch and Lin [103], Shingal and Lin [46], Meng *et al.* [47,48], Fritsch [49], Corchs *et al.* [105], Schultz *et al.* [106], Kuang and Lin [64], Busnego *et al.* [104], and unpublished data from Pons [50], obtained with the semiclassical counterpart of our effective Hamiltonian method); and experiment (Williams *et al.* [107], deHeer *et al.* [108], Shah *et al.* [94,109,56], Slachter *et al.* [102], and Graham *et al.* [110]). Overall agreement is good, and slighly better for $\overline{\sigma}$; hence, these recommended data for the single-electron processes are given in Table IV. In addition, several points deserve discussion.

First, and as mentioned in Sec. II B, it is reasonable to display our data together with an estimation of anisotropy effects. These ''error bars'' can be gauged from the difference between our results for σ [eq. (11)], obtained with the origin of the effective Coulomb potential at the midpoint of the H-H axis, and $\overline{\sigma}$ [Eq. (12)], calculated with the approximate orientation averaging described in Sec. II B. We see in Figs. 6 and 7 that the relative error bars are small, and diminish with the ion charge q. In addition, although for ionization there are no semiclassical results to compare our cross sections with, the comparison for single-electron capture (Fig. 7) is very good, even for H^+ projectiles, and for He^{2+} our estimates are systematically closer to experiment [109,56], to the model close-coupling results of Fritsch [49], and to the new perturbative values from Busnengo *et al.* [104], than to the earlier unitarized close-coupling results of Shingal and Lin [46] or to previous estimates from Corchs *et al.* [105].

On the other hand, the comparison is more difficult when the measured data include contributions from two-electron processes (see Sec. II B). At large v, our small discrepancies with the measurements for ionization could be attributed to our overestimation of the cross section for double ionization $\overline{\sigma}_{di}$. The situation is worst for Li^{3+} projectiles, for which measurements include a contribution from transfer ioniza-

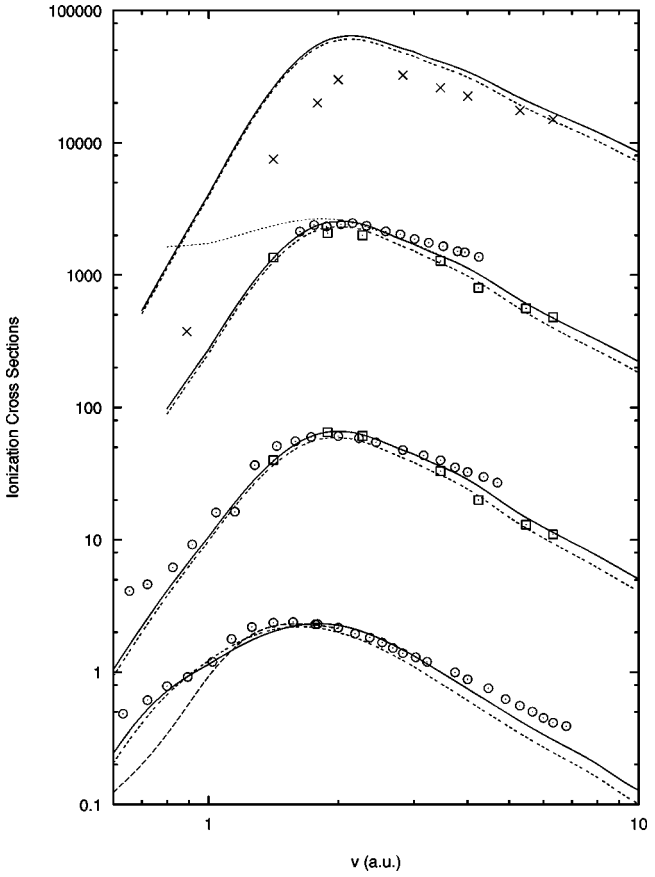

FIG. 6. We draw, as functions of the relative velocity v, the ionization cross sections for $A^{q+}+H_2$ collisions (in units of 10^{-16} cm^2 and scaled as stated below), obtained from our calculations using the method of Sec. II B. The difference between our values for $\overline{\sigma}(v)$ (——) [Eq. (12)] and $\sigma(v)$ (--- ---) [Eq. (11)] are taken, as explained in that section, as estimating the anisotropy effects. We compare our results with the following experimental and theoretical data. For H^+ projectiles: single plus double ionization: (⊙) measurements from Shah *et al.* [109,56]; (— — —) data from Pons [50]. For He^{2+} projectiles, single plus double ionization (data×10): (⊙) measurements from Shah *et al.* [109,56]; (□) data from Meng *et al.* [47,48]. For Li^{3+} projectiles, single, double, and transfer ionization (data×200): (· · · ·) present results with the autoionization contribution: (⊙) measurements from Shah *et al.* [94,109]; (□) data from Meng *et al.* [47,48]. For Be^{4+} projectiles, single ionization (data×5000): (×) results from Schultz *et al.* [106].

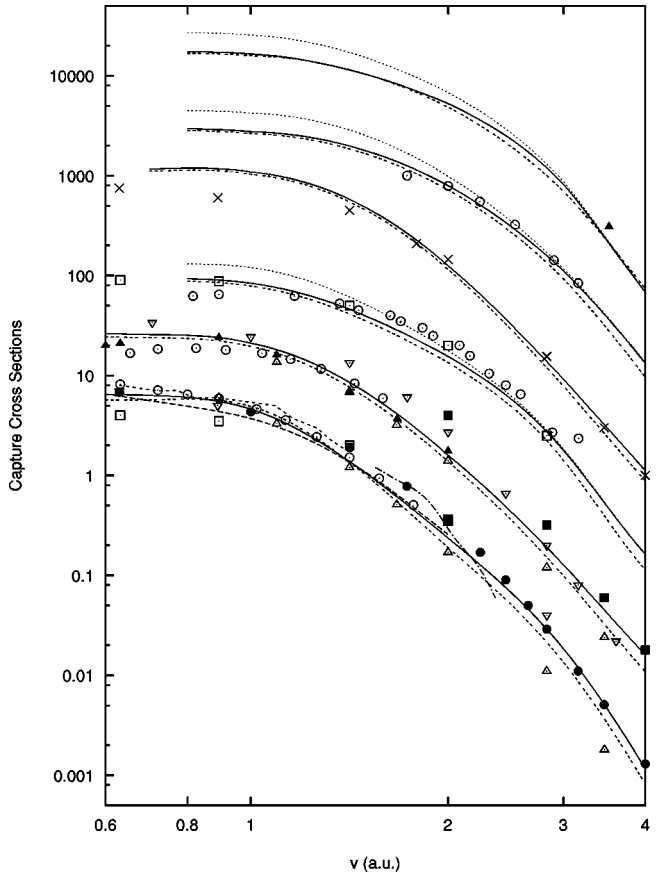

FIG. 7. We draw, as functions of the relative velocity v, the capture cross sections for $A^{q+}+H_2$ collisions (in units of 10^{-16} cm^2 and scaled as stated below), obtained from our calculations using the method of Sec. II B. The difference between our values for $\overline{\sigma}(v)$ (——) [Eq. (12)] and $\sigma(v)$ (--- ---) [Eq. (11)] are taken, as explained in that section, as estimating the anisotropy effects. We compare our results with the following experimental and theoretical data. For H^+ projectiles, single capture: measurements of (— · — · — · —) de Heer *et al.* [108], (– – – –) Williams and Dunbar [107], and (⊙) Shah *et al.* [109,56]; (— — —) results from Pons [50], (△) Busnengo *et al.* [104], (▽) Shingal and Lin [46], (□) Meng *et al.* [47,48], (●) Kuang and Lin [64]. For He^{2+} projectiles, single capture (data×2): (⊙) measurements of Shah *et al.* [109,56]; calculations of (▽) Shingal and Lin [46], (full triangle) Fritsch [49], (full box) Corchs *et al.* [105], (△) Busnengo *et al.* [104]. For Li^{3+} projectiles, single capture plus transfer ionization (data×5): (· · · ·) present results with the autoionization contribution; (⊙) measurements of Shah *et al.* [94,109]; (□) results from Meng *et al.* [47,48]. For Be^{4+} projectiles, single capture (data×50): (×) results from Schultz *et al.* [106]. For B^{5+} projectiles, single capture plus transfer ionization (data×200): (· · · ·) present results with the autoionization contribution: (⊙) measurements of Shah *et al.* [71]. For C^{6+} projectiles, single capture plus transfer ionization (data×500): (· · · ·) present results with the autoionization contribution; (full triangle up) measurements of Graham *et al.* [110].

tion, both from direct processes and from autoionization of the doubly excited $(Li^+)^{**}$ ion. We have checked, using CTMC [9] and semiclassical [50] methods, that the IPM considerably overestimates these contributions. Consequently, for Li^{3+}, comparison with experiment does not yield, for $v<2$ a.u., a fair estimate of the accuracy of our single-electron data, and we give in Figs. 6 and 7 our results with and without $\overline{\sigma}_{ti}$; for conciseness, the former are displayed only for the orientation-averaged calculations. We have also included in the figures the CTMC data from Meng *et al.* [47], who also employ a factorized electron distribution (hence an IPM), and include the transfer ionization contribution; we are unable to explain the coincidence between their data with the contribution and our results without it. Finally, we attribute the large differences with the CTMC results of Schultz *et al.* [106] for Be^{4+} projectiles to their use of a microcanonical initial condition, which, as usual, considerably underestimates the cross sections at low v.

2. Scaling rules

The usefulness of scaling rules for H_2 targets follows as for $H(1s)$. Our procedure in this case is more empirical than in Sec. III A, because at large v the ionization cross sections for molecular targets do not follow a simple rule like Eq. (13), and, in particular, we do not obtain $\overline{\sigma}_{si} \propto q^2$. We have examined this point, and found that the single-electron ionization probabilities do obey the same laws as for H targets: mainly $\wp_i(v,b,q) \propto q$ for fixed $v, bq^{-1/2}$ and for the impact parameters b that determine the cross sections. However, for these impact parameters, the probability $\wp_e(v,b,q)$ of the electron not being captured or ionized strongly diminishes with q, so that, for the range of nuclear velocities considered here, no simple scaling exists, even at high v, for the combined probability $P_{si} = 2\wp_i\wp_e$ [eq. (7)]. Our empirical law for $\overline{\sigma}_{si}$ is

$$\overline{\sigma}_{si}^{\text{scaled}}(q,v) = \sigma(1,v) q^{2\{0.92 - \exp[-0.57(v-0.01q)] - \exp[-1.8(v^2-0.08q)]\}}. \tag{16}$$

The accuracy of this analytical fit is slightly worse than for the ion-atom case. For $v \geq 0.5$ a.u., the maximum absolute error of this expression with respect to our calculated values is about $0.2q^2$, in the maximum region of the cross section.

On the other hand, with regard to electron capture, we found a simple, linear scaling rule for $\overline{\sigma}_{sc}$:

$$\overline{\sigma}_{sc}^{\text{scaled}}(q,v) = \overline{\sigma}_{sc}(1,v')q \tag{17}$$

with $v' = vq^{0.11}$. As in Sec. III A, an estimate of the accuracy of this expression is difficult, and may be given by the largest absolute error with respect to our calculated values of σ_c; this is, at low v, of the order of $0.6q$ (for $q=8$).

3. Application of our data to dressed projectiles

As for the ion-atom case, we check in this section whether the results for bare ion projectiles can be used to estimate, for $v > 1$ a.u., the corresponding data for dressed projectiles with the same net charge q. Then, the scaling laws of Eqs. (16) and (17) can be applied to reactions that have not been treated experimentally, such as for Be^{q+} $(q=2,3)$ projectiles, or for impact by dressed ions A^{q+} with $q>4$ (ionization) and 5 (capture).

We display in Figs. 8 and 9 the same capture and ionization data given in Figs. 6 and 7, respectively, together with the corresponding measurements from Shah *et al.* [94,71,91,95] for bare and dressed-ion projectiles colliding with H_2. The comparison is very similar to that for atomic targets (Sec. III A), and the discussion on the influence of the core electrons, which follows similar lines, will not be repeated. Incidentally, a fortuitous agreement at low v should be noted between our ionization data with the autoionization contribution and experiment for dressed ions with $q=2$; this is due to a compensation between our overestimation of the double-capture cross section (Sec. II B) and our underestimation of the role of the core (Sec. III A).

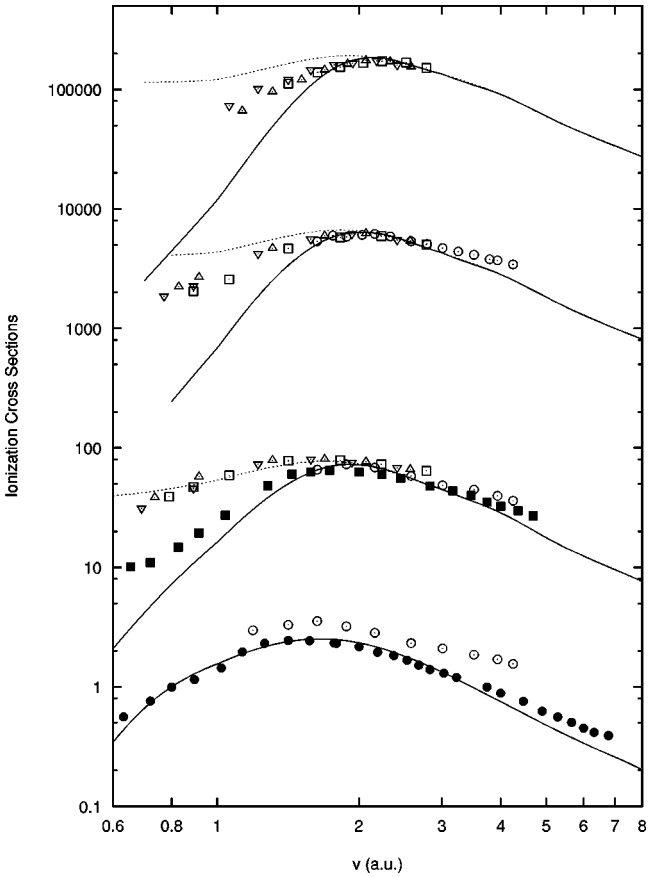

FIG. 8. Comparison of the present results $\overline{\sigma}(v)$ without (——) and with (· · · ·) autoionization contributions (in units of 10^{-16} cm^2 and scaled as stated below), for the single, double, and transfer ionization cross section of $A^{q+} + H(1s)$ collisions, with A^{q+} a bare ion, with experimental data for stripped and dressed A^{q+} projectiles. $q=1$: data from Shah *et al.* for H^+ [109,56] (●) and Li^+ [94] (⊙). $q=2$ (data×10): values from Shah *et al.* for He^{2+} [109,56] (full box), Li^{2+} [94] (⊙), C^{2+} [109] (□), N^{2+} [109] (△), and O^{2+} [109] (▽). $q=3$ (data×500): values from Shah *et al.* for Li^{3+} [94] (⊙), C^{3+} [109] (□), N^{3+} [109] (△), and O^{3+} [109] (▽). $q=4$ (data×10 000): values from Shah *et al.* [109] for C^{4+} (□), N^{4+} (△), and O^{4+} (▽).

IV. CONCLUSIONS

We have reported results for single-electron ionization and capture cross sections in $A^{q+} + H$ collisions, with A^{q+} a bare ion, in a wide range of intermediate energies. Use of an impact parameter, CTMC treatment, with initial spatial and momentum densities that are close to the exact ones [25], achieves a considerable improvement over previous classical work, so that the accuracy of the approach is much higher than usually assumed [1,2]. This applies, to a good extent, to partial cross sections as well as transition probabilities, although tabulation of the former quantities exceeds the aims of the present paper. This performance of CTMC calculations is very encouraging, since they are considerably simpler than *ab initio*, close-coupling treatments, especially when pseudostates need to be included in the latter (see, e.g., Refs. [112–114,2,64,55,54]); also, as we have seen, perturbative approaches are not applicable in the lower range of nuclear velocities that we have treated. Our data for H targets are of predictive value for bare A^{q+} ions, $q>3, v>3$ a.u.,

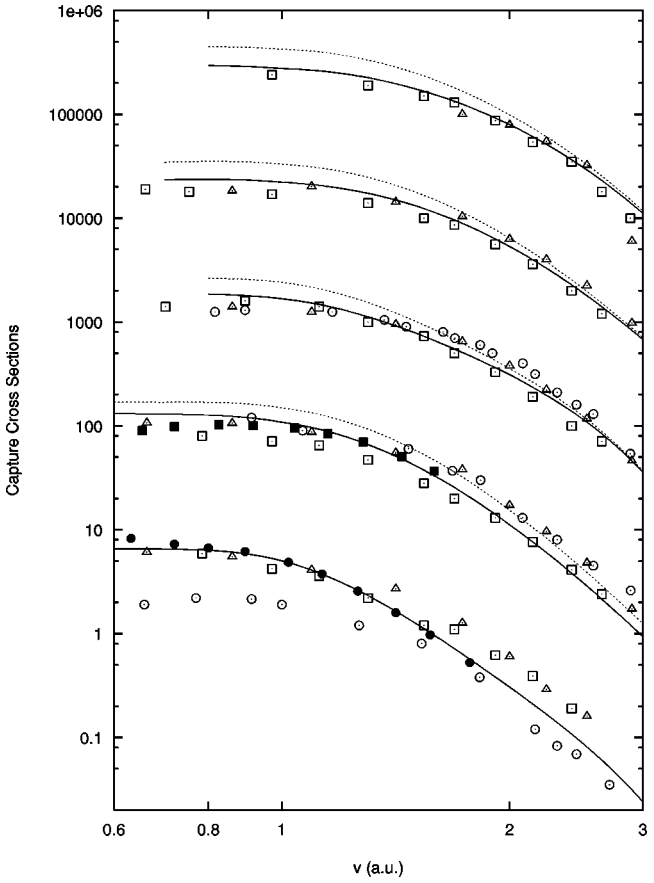

FIG. 9. Comparison of the present results $\overline{\sigma}(v)$ without (——) and with (· · · ·) autoionization contributions (in units of 10^{-16} cm^2 and scaled as stated below), for the single capture plus transfer ionization cross section of $A^{q+}+\mathrm{H}(1s)$ collisions, with A^{q+} a bare ion, with experimental data for stripped and dressed A^{q+} projectiles. $q=1$: measurements from Shah *et al.* for H^+ [109,56] (●), Li^+ [71] (⊙), B^+ [71] (△), and C^+ [71] (□). $q=2$ (data×10): values from Shah *et al.* for He^{2+} [109,56] (full box), Li^{2+} [94] (⊙), B^{2+} [71] (△), and C^{2+} [71] (□). $q=3$ (data×100): values from Shah *et al.* for Li^{3+} [94] (⊙), B^{3+}, [71] (△), and C^{3+} [71] (□). $q=4$ (data×1000): values from Shah *et al.* [71] for B^{4+} (△) and C^{4+} (□). $q=5$ (data ×10 000): values from Shah *et al.* [71] for B^{5+} (△) and C^{5+} (□).

and at low v we compare very well with close-coupling results for ionization. In this respect, we have mentioned that the problem of the normalization of the experiment by proton impact cannot be taken as being completely solved—otherwise, we would have a surprising coincidence of classical and semiclassical results lying above the measurements at the cross-section maximum. For capture, our data lie systematically above those of atomic treatments, and this is a matter worth investigating, since we agree at the higher v with CDW results.

In the present work, we have also checked that our previous studies of the mechanisms [7,8] extend to projectiles other than He^{2+}. We have then reckoned that the detailed inner structure of either colliding partner may not be of paramount importance to treat ionization and capture processes, since these take place outside the inner regions. We were thus led to compare our data for bare ion impact to the experiment for dressed-ion projectiles, showing that core effects are unimportant for nuclear charges $Z>1$ and a fixed net charge q, at $v>0.5$ a.u. (capture) and $v>1.5$ a.u. (ionization), where our estimates are of predictive value for $q>5$, and Be^{q+} impact. At smaller velocities, simple arguments indicate that electron correlation effects are at work, and these must involve, for ionization, the saddle-point mechanism, which is also a point that deserves further investigation.

From the previous conclusions on the mechanisms, there also emerges a model for H_2 targets, in which the relevant quantities are the vertical ionization potential of the molecule and the projectile net charge q. This apparently crude model yields, as far as we know, the most accurate theoretical data for single-electron processes, in a v domain spanning the maximum of the ionization cross section. On the other hand, as in other simplified approaches [49,48,38], dissociative reactions cannot be separated from nondissociative events, and the model fails for double-electron processes, and especially with respect to transfer ionization stemming from autoionization. Therefore, only the cross sections for single ionization and capture are given in tabulated form. Comparison between Table I (for H targets) and Table IV (for H_2) then shows that, because of a compensation effect at low v, the data for atomic and molecular targets are of the same order, while at large v the latter tend to twice the former, as assumed in previous works. Comparison with experiment is very encouraging, except that our limitation to single-electron events causes an inconvenience for Li^{3+} projectiles at low v, because the measured data [94,109] include transfer ionization. Nevertheless, it should be remembered that one of the aims of the present work was to check whether the method provides reliable data for the single-electron cross sections, rather than to reproduce those of all the experiments. Our results are of predictive value for Be^{q+} ($q=2,3,4$) projectiles and for impact by dressed ions A^{q+} with $q>4$ (ionization) and $q>5$ (capture), hence including, in particular, the important [5,4] carbon and oxygen ions.

For application purposes, Eqs. (14), (15), (16), and (17) provide a scaling of our data to a benchmark case, which is that of H^+ impact, except for electron capture from H targets, where the benchmark is He^{2+}. To construct these empirical laws, we have studied the variation of the transition probabilities with q, v, and the impact parameter b. We have found for ionization of H targets that the Born-type $\propto q^2$ variation holds even at such low v that the conditions for the Born approximation are inapplicable. This behavior can be related to a scaling of the ionization probabilities, related to a distant collision hypothesis for the direct ionization mechanism. With respect to the variation with v, our classical data are compatible, for $v \geqslant 5$ a.u., with a Bethe-Born limit behavior (13). Similar behaviors are found for the single-electron probabilities for ionization of the ''active'' electron in collisions with H_2 targets, but not to the total single ionization probabilities, because of the variation in the transition probability of the ''passive'' electron.

ACKNOWLEDGMENTS

This work has been partially supported by DGICYT PB96-0056, and the project ENRESA 0703240. We thank Professor M. B. Shah for his helpful comments.

[1] N. Stolterfoht, R. D. DuBois, and R. D. Rivarola, *Electron Emission in Heavy Ion-Atom Collisions* (Springer Verlag, Berlin, 1997).
[2] B. H. Bransden and M. H. C. McDowell, *Charge Exchange and the Theory of Ion-Atom Collisions* (Oxford Science Publications, Oxford, 1992).
[3] H.B. Gilbody, Adv. At. Mol. Phys. **22**, 143 (1986).
[4] Europhys. News, Nov./Dec. 1998, Fusion Special Issue.
[5] H.B. Gilbody, Adv. At., Mol., Opt. Phys. **32**, 149 (1994).
[6] R. Moshammer, I. Ullrich, M. Unverzagt, W. Schmidt, P. Jardin, R.E. Olson, R. Mann, R. Dörner, V. Mergel, U. Buck, and H. Schmidt-Böcking, Phys. Rev. Lett. **73**, 3371 (1994).
[7] C. Illescas, I. Rabadán, and A. Riera, J. Phys. B **30**, 1765 (1997).
[8] C. Illescas, I. Rabadán, and A. Riera, Phys. Rev. A **57**, 1809 (1998).
[9] C. Illescas and A. Riera, J. Phys. B **31**, 2777 (1998).
[10] C. Illescas and A. Riera, Phys. Rev. Lett. **76**, 1043 (1998).
[11] R. Abrines and I.C. Percival, Proc. Phys. Soc. London **88**, 861 (1966).
[12] R.E. Olson and A. Salop, Phys. Rev. A **16**, 531 (1977).
[13] D.L. Bunker, Methods Comput. Phys. **10**, 287 (1971).
[14] I.C. Percival and D. Richards, Adv. At. Mol. Phys. **11**, 1 (1973).
[15] L.G.J. Boesten, T.F.M. Bonsen, and D. Banks, J. Phys. B **8**, 628 (1975).
[16] S.L. Willis, G. Peach, M.R.C. McDowell, and J. Banerji, J. Phys. B **18**, 3939 (1985).
[17] G. Schiwietz and W. Fritsch, J. Phys. B **20**, 5463 (1987).
[18] C.O. Reinhold and C.A. Falcón, J. Phys. B **21**, 1829 (1988).
[19] C.O. Reinhold and J. Burgdörfer, J. Phys. B **26**, 3101 (1993).
[20] P.L. Grande and G. Schiwietz, J. Phys. B **28**, 425 (1995).
[21] S. Keller, H. Ast, and R.M. Dreizler, J. Phys. B **26**, L737 (1993).
[22] B.H. Bransden and R.K. Janev, Adv. At. Mol. Phys. **19**, 1 (1983).
[23] G.H. Gillespie, J. Phys. B **15**, L729 (1982).
[24] D. Eichenauer, N. Grun, and W. Scheid, J. Phys. B **14**, 3929 (1981).
[25] D.J.W. Hardie and R.E. Olson, J. Phys. B **16**, 1983 (1983).
[26] J.S. Cohen, J. Phys. B **18**, 1759 (1985).
[27] C.J. Wood, C.R. Feeler, and R.E. Olson, Phys. Rev. A **56**, 3701 (1997).
[28] C. Illescas and A. Riera, Phys. Scr. **T80**, 420 (1999).
[29] N. Toshima, T. Ishihara, A. Ohsaki, and T. Watanabe, Phys. Rev. A **40**, 2192 (1989).
[30] T. Adachi and T. Kotani, Prog. Theor. Phys. Suppl., commemorative issue for the 30th anniversary of the Meson Theory by Yukawa (1965), p. 316.
[31] T. Adachi and T. Kotani, Prog. Theor. Phys. Suppl. **39**, 430 (1968).
[32] T. Adachi and T. Kotani, Prog. Theor. Phys. Suppl. **39**, 785 (1968).
[33] J.S. Burlisch and J. Stoer, Numer. Math. **8**, 1 (1966).
[34] G. Bandarage and R. Parson, Phys. Rev. A **41**, 5878 (1990).
[35] R.E. Olson, Phys. Rev. A **27**, 1871 (1983).
[36] L.F. Errea, J.D. Gorfinkiel, A. Macías, L. Méndez, and A. Riera, J. Phys. B **30**, 3855 (1997).
[37] A. Macías, L.F. Errea, J.D. Gorfinkiel, L. Méndez, and A. Riera, J. Mol. Struct.: THEOCHEM **433**, 169 (1998).
[38] D. Elizaga, L.F. Errea, J.D. Gorfinkiel, C. Illescas, A. Macías, L. Méndez, A. Riera, A. Rojas, R.M. Dreizler, A. Henne, T. Kirchner, O. Kroneisen, and H.J. Lüdde, J. Phys. B **32**, 857 (1999).
[39] L.F. Errea, J.D. Gorfinkiel, A. Macías, L. Méndez, and A. Riera, J. Phys. B **32**, 1705 (1999).
[40] L. F. Errea, A. Macías, L. Méndez, and A. Riera, J. Phys. B **32**, 4065 (1999).
[41] C.F. Giese and W.R. Gentry, Phys. Rev. A **10**, 2156 (1974).
[42] R. Prosmiti, O.L. Polyansky, and J. Tennyson, Chem. Phys. Lett. **273**, 107 (1997).
[43] D. Elizaga D, L. F. Errea, and A. Rojas (private communication).
[44] J.H. McGuire and L. Weaver, Phys. Rev. A **16**, 41 (1977).
[45] V.A. Sidorovitch, J. Phys. B **14**, 4805 (1981).
[46] R. Shingal and C.D. Lin, Phys. Rev. A **40**, 1302 (1989).
[47] L. Meng, C.O. Reinhold, and R.E. Olson, Phys. Rev. A **40**, 3637 (1989).
[48] L. Meng, C.O. Reinhold, and R.E. Olson, Phys. Rev. A **42**, 5286 (1990).
[49] W. Fritsch, Phys. Rev. A **46**, 3910 (1992).
[50] B. Pons (private communication).
[51] Y.D. Wang, C.D. Lin, N. Toshima, and Z. Chen, Phys. Rev. A **52**, 2852 (1995).
[52] M. McCartney, J. Phys. B **30**, L155 (1997).
[53] N. Toshima, Phys. Rev. A **50**, 3940 (1994).
[54] N. Toshima, Phys. Rev. A **59**, 1981 (1999).
[55] L.F. Errea, C. Harel, C. Illescas, H. Jouin, L. Méndez, B. Pons, and A. Riera, J. Phys. B **31**, 3199 (1998).
[56] M.B. Shah, P. McCallion, and H.B. Gilbody, J. Phys. B **22**, 3983 (1989).
[57] M.B. Shah, J. Geddes, M.M. McLaughlin, and H.B. Gilbody, J. Phys. B **31**, L757 (1998).
[58] D.R. Bates and G.W. Griffing, Proc. R. Soc. London, Ser. A **66**, 961 (1953).
[59] G.W. McClure, Phys. Rev. **148**, 47 (1966).
[60] M.B. Shah and H.B. Gilbody, J. Phys. B **14**, 2361 (1981).
[61] M.B. Shah, D.S. Elliot, P. McCallion, and H.B. Gilbody, J. Phys. B **21**, 2455 (1988).
[62] T.G. Winter, Phys. Rev. A **25**, 697 (1982).
[63] T.G. Winter, Phys. Rev. A **37**, 4656 (1988).
[64] J. Kuang and C.D. Lin, J. Phys. B **30**, 101 (1997).
[65] D.S.F. Crothers, J. Phys. B **15**, 2061 (1982).
[66] D.S.F. Crothers and J.F. McCann, J. Phys. B **16**, 3229 (1983).
[67] B.H. Bransden, C.W. Newby, and C.J. Noble, J. Phys. B **13**, 4245 (1980).
[68] M.S. Gravielle and J.E. Miraglia, Phys. Rev. A **51**, 2131 (1995).
[69] H.J. Lüdde and R.M. Dreizler, J. Phys. B **15**, 2713 (1982).
[70] K. Wada and T. Murai, J. Phys. B **18**, 4259 (1985).
[71] T.V. Goffe, M.B. Shah, and H.B. Gilbody, J. Phys. B **12**, 3763 (1979).
[72] R.L. Becker and A.D. McKeller, J. Phys. B **17**, 3923 (1984).
[73] R.E. Olson, Phys. Rev. A **24**, 1726 (1981).
[74] J. Pascale, C.O. Reinhold, and R.E. Olson, Phys. Rev. A **42**, 5305 (1990).
[75] C. Laulhé, E. Jacquet, P. Boduch, M. Chantepie, N. Ghérard, H. Huson, D. Lecler, and J. Pascale, J. Phys. B **30**, 2897 (1997).
[76] C. Harel, H. Jouin, and B. Pons, At. Data Nucl. Data Tables **68**, 279 (1998).
[77] L.F. Errea, C. Harel, H. Jouin, L. Méndez, B. Pons, and A.

Riera, J. Phys. B **27**, 3603 (1994).
[78] R.K. Janev and H.P. Winter, Phys. Rep. **5**, 265 (1985).
[79] V.D. Rodríguez and C.A. Falcón, J. Phys. B **23**, L547 (1990).
[80] N. F. Mott and H. S. W. Massey, *The Theory of Atomic Collisions* (Clarendon, Oxford, 1965).
[81] N. Bohr, K. Dan. Vidensk. Selsk. Mat. Fys. Medd. **18**, 8 (1948).
[82] J.M. Hansteen, Adv. At. Mol. Phys. **11**, 299 (1975).
[83] A.B. Voitkiv and V.A. Pazdzersky, J. Phys. B **21**, 3369 (1988).
[84] W. Fritsch and K.H. Schartner, Phys. Lett. A **126**, 17 (1987).
[85] V.D. Rodríguez and J.E. Miraglia, Phys. Lett. A **138**, 123 (1989).
[86] H. Ryufuku and T. Watanabe, Phys. Rev. A **18**, 2005 (1978).
[87] H. Ryukufu and T. Watanabe, Phys. Rev. A **19**, 1538 (1979).
[88] H. Ryufuku, Phys. Rev. A **25**, 733 (1982).
[89] D.S.F. Crothers and N.R. Todd, J. Phys. B **13**, 545 (1980).
[90] R.K. Janev and L.P. Presnyakov, Phys. Rep. **70**, 1 (1981).
[91] M.B. Shah and H.B. Gilbody, J. Phys. B **14**, 2831 (1981).
[92] J. S. Briggs and K. Taulbjerg, in *Structure and Collisions of Ions and Atoms*, edited by A. Sellin, Topics in Current Physics Vol. 5 (Springer, Berlin, 1978), p. 105.
[93] J.H. McGuire, N. Stolterfoht, and P.R. Simony, Phys. Rev. A **24**, 97 (1981).
[94] M.B. Shah, T.V. Goffe, and H.B. Gilbody, J. Phys. B **11**, L233 (1978).
[95] M.B. Shah and H.B. Gilbody, J. Phys. B **15**, 413 (1982).
[96] M.B. Shah and H.B. Gilbody, J. Phys. B **16**, 4395 (1983).
[97] W.A. Beck and L. Wilets, Phys. Rev. A **55**, 2821 (1997).
[98] J.H. McGuire, Phys. Rev. Lett. **49**, 1153 (1981).
[99] J.H. McGuire, Phys. Rev. A **36**, 1114 (1987).
[100] N. Stolterfoht, Nucl. Instrum. Methods Phys. Res. B **53**, 477 (1991).
[101] R.E. Olson, K.H. Berkner, W.G. Graham, R.V. Pyle, A.S. Slachter, and J.W. Stearns, Phys. Rev. Lett. **41**, 163 (1978).
[102] A.S. Slachter, K.H. Berkner, W.G. Graham, R.V. Pyle, J.W. Stearns, and J.A. Tanis, Phys. Rev. A **24**, 1110 (1981).
[103] W. Fritsch and C.D. Lin, Phys. Rev. A **29**, 3039 (1984).
[104] H.F. Busnengo, S.E. Corchs, and R.D. Rivarola, Phys. Rev. A **57**, 2701 (1998).
[105] S.E. Corchs, R.D. Rivarola, J.H. McGuire, and Y.D. Wang, Phys. Scr. **50**, 469 (1994).
[106] D.R. Schultz, P.S. Krstić, and C.O. Reinhold, Phys. Scr. **T62**, 69 (1996).
[107] J.F. Williams and D.N.F. Dunbar, Phys. Rev. **62**, 149 (1966).
[108] F.J. de Heer, J. Schutten, and H. Moustafa, Physica (Amsterdam) **32**, 177 (1966).
[109] M.B. Shah and H.B. Gilbody, J. Phys. B **15**, 3441 (1982).
[110] W.G. Graham, K.H. Berkner, R.V. Pyle, A.S. Schlachter, J.W. Stearns, and J.A. Tanis, Phys. Rev. A **30**, 722 (1984).
[111] R.K. Janev, G. Ivanovsky, and E.A. Solov'ev, Phys. Rev. A **49**, R645 (1994).
[112] J. Reading, A.L. Ford, G.L. Swafford, and A. Fitchard, Phys. Rev. A **20**, 130 (1979).
[113] J. Reading and A.L. Ford, J. Phys. B **12**, 1367 (1979).
[114] G. Bandarage and W.R. Thorson, Phys. Rev. A **37**, 716 (1988).